

- [12] D. P. Akitt, R. J. Strain, P. D. Coleman, "Millimeter Wave Generation by Nonlinear Quantum Susceptibility," presented at 6.6, Millimeter and Submillimeter Conf., Orlando, Fla.; January, 1963.
- [13] J. R. Fontana, R. H. Pantell, R. G. Smith, "Harmonic generation using the ammonia inversion transition," Proc. IRE (Correspondence), vol. 50, pp. 469-470; April, 1962.
- [14] C. M. Kellington, "Resonant harmonic generation in ruby," Phys. Rev. Lett., vol. 9, pp. 57-58; July 15, 1962.
- [15] A. Javan and C. H. Townes, "Quarterly Progress Report No. 66," M.I.T. Research Lab. of Electronics, Cambridge, Mass.; July 15, 1962.
- [16] A. Javan, "Transitions a plusieurs quanta et amplification maser dans les systemes a deux niveaux," *Le Journal de Physique et le Radium*, vol. 19, pp. 806-808; November, 1958.
- [17] T. Yajima and Koichi Shimoda, "Multiple quantum effect in a three-level gas maser," in "Advances in Quantum Electronics," J. R. Singer, Ed., Columbia University Press, New York, N. Y., 1961.
- [18] T. Yajima, "Three-level maser action in a gas, I. theory of multiple quantum transition and Doppler effect in three-level gas maser, II. Experimental study on formic acid," *J. Phys. Soc. Japan*, vol. 16, pp. 1594-1606, August, 1961; vol. 16, pp. 1709-1718, September, 1961.
- [19] E. J. Woodbury and W. K. Ng, "Ruby laser operation in the near IR," Proc. IRE (Correspondence), vol. 50, p. 2367; November, 1962.
- [20] G. Eckhardt, R. W. Hellwarth, F. J. McClung, S. E. Schwarz, D. Weiner, and E. J. Woodbury, "Stimulated Raman scattering from organic liquids," Phys. Rev. Lett., vol. 9, p. 455; 1962.

## TE<sub>01</sub> Mode Components in the 3-mm Region\*

ALAN J. SIMMONS†, SENIOR MEMBER, IEEE

**Summary**—In the 3-mm region (94 Gc) it is desirable to use waveguide components operating in the low loss TE<sub>01</sub> mode in circular waveguide rather than in fundamental-mode rectangular waveguide. Because this is a higher mode, mode purity is of major concern. A method of identifying undesired modes and their amplitudes is by means of radiation patterns from the end of the waveguide.

Components developed to operate in this mode include a transition from rectangular to circular waveguide, standing wave detector, variable attenuator, directional coupler, flexible waveguide, fixed 90° bend and rotary joint.

### INTRODUCTION

TRANSMISSION of millimeter-wave energy by means of the TE<sub>01</sub> mode has the advantage over fundamental-mode rectangular waveguide of lower loss, greater power capacity, larger size and simpler flange couplings. It has the advantage over optical or quasi-optical transmission lines of being a closed shielded system with controllable single-mode propagation which permits launching of the mode with high efficiency. Potential use of this mode has been boosted by recent development of high-power magnetrons whose output is in this mode, and which develop enough power to cause RF breakdown in standard air-filled rectangular waveguide at atmospheric pressure.<sup>1</sup>

\* Received January 21, 1963. Revised manuscript received April 5, 1963. This work was sponsored by the U. S. Army Signal Research and Development Laboratory, Fort Monmouth, N. J. under Contract No. DA-36-039-sc-88979. This paper was presented at the Millimeter and Submillimeter Conference, Orlando, Fla., January 7-10, 1963.

† Technical Research Group, Inc., East Boston, Mass.

<sup>1</sup> "Inverted coaxial magnetron delivers 100 kw at K<sub>a</sub>-band," *Microwaves*, pp. 46-47; March, 1962.

This paper describes the development of components to operate in the TE<sub>01</sub> mode in the frequency region around 94 Gc (3.2 mm), which is in the neighborhood of a propagation window in the earth's atmosphere.

The components developed or under development in this program include the following:

- 1) transition from rectangular to circular waveguide
- 2) mode filter
- 3) 90° bends
- 4) 10-db directional couplers to rectangular waveguide
- 5) flexible sections
- 6) standing wave detector
- 7) variable attenuator
- 8) low- and high-power terminations
- 9) manual three-port RF switch
- 10) rotary joint
- 11) coupling flanges
- 12) pressurizing window sections

Most of this paper will be concerned with items 6) and 7) which have certain novel features and represent major design problems. A brief description of the method of design and results achieved on some of the other components will be presented.

The inner diameter of the circular waveguide used is 0.250 inch; cutoff frequency for the TE<sub>01</sub> mode is 57.5

Gc, for the TE<sub>02</sub> mode, 105 Gc. There are a total of ten modes which can propagate in this size waveguide in the five per cent band centered at 93.75 Gc, and one of the primary problems is to avoid excitation of any but the desired TE<sub>01</sub> mode.

#### MODE PURITY

Mode purity is defined as the ratio of power in the TE<sub>01</sub> mode to power in all other undesired modes. In the presence of many modes of unknown amplitude, phase and orientation, it is difficult to obtain a simple, straightforward and unambiguous measurement of mode purity. A number of in-waveguide methods have been used<sup>2,3</sup> for mode-purity measurement. These involve either probing of the field components in the neighborhood of

that only single-mode fields are present in the aperture, that is, that the aperture discontinuity causes no cross coupling between modes. Using this theory and, in addition, making the assumption that the reflection coefficient for all modes at the aperture is small (this assumption is quite justified for the waveguide diameters considered here for the TE<sub>01</sub> mode and for modes with lower cutoff frequencies),<sup>6</sup> expressions for the electric field patterns of the various modes have been derived. These expressions have all been normalized for unit power so that the field strength amplitudes for the different modes may be directly compared. In spherical coordinates (see Fig. 1) the field components are:

a) *TM<sub>mn</sub> Modes:*

$$|E_\theta| = A_{mn} \frac{\sin \theta \left[ \left( 1 - \left( \frac{f_c}{f} \right)^2 \right)^{1/2} + \cos \theta \right] J_m(ka \sin \theta) \cos m\phi}{\sin^2 \theta - \left( \frac{f_c}{f} \right)^2}, \quad (1)$$

b) *TE<sub>mn</sub> Modes:*

$$|E_\theta| = B_{mn} \frac{m \left[ 1 + \cos \theta \left( 1 - \left( \frac{f_c}{f} \right)^2 \right)^{1/2} \right] J_m(ka \sin \theta) \sin m\phi}{\left( \frac{f_c}{f} \right)^2 - \sin^2 \theta}, \quad (2)$$

$$|E_\phi| = B_{mn} \frac{\left[ \left( 1 - \left( \frac{f_c}{f} \right)^2 \right)^{1/2} + \cos \theta \right] J_m'(ka \sin \theta) \cos m\phi}{\left( \frac{f_c}{f} \right)^2 - \sin^2 \theta}, \quad (3)$$

the waveguide wall, or selective multihole coupling devices, or methods which make use of resonance techniques. A new method which we have found useful is one in which the circular pipe is allowed to radiate from its open end and the measured radiation patterns are compared with theoretical radiation patterns. Such a method has also recently been described by Müller.<sup>4</sup>

The theoretical radiation pattern of the circular waveguide aperture is given by Silver in "Microwave Antenna Theory and Design,"<sup>5</sup> in which it is assumed

<sup>2</sup> H. G. Effemey, "A survey of methods used to identify fields or wave modes in cylindrical waveguide," *Proc. IEE*, vol. 106, pp. 75-83; January, 1959.

<sup>3</sup> Y. Klinger, "The measurement of spurious modes in over-moded waveguides," *Proc. IEE*, vol. 106, pp. 89-93; 1900.

<sup>4</sup> K. E. Müller, "Über den Nachweis höherer Schwingungsformen in Hohlleitern mit Hilfe des Strahlungsfeldes," *Nachrichtentechnik*, vol. 12, pp. 18-24; January, 1962.

<sup>5</sup> Samuel Silver, "Microwave antenna theory and design," Rad. Laboratory Series, L. N. Ridenour Ed., McGraw-Hill Book Co., Inc., New York, N. Y., vol. 12; 1949. See sect. 10.2.

where

$$A_{mn} = \left[ \frac{120}{\left[ 1 - \left( \frac{f_c}{f} \right)^2 \right]^{1/2}} \right]^{1/2};$$

$$B_{mn} = \frac{f_c}{f} \frac{A_{mn}}{\left[ 1 - \left( \frac{mf}{kaf_c} \right)^2 \right]^{1/2}};$$

$$k = 2\pi/\lambda;$$

$$a = \text{waveguide radius};$$

$$f_c = \text{cutoff frequency of the } mn\text{th mode};$$

$$f = \text{frequency};$$

*J<sub>m</sub>* and *J<sub>m'</sub>* = Bessel functions of the first kind, and their derivatives, respectively.

<sup>6</sup> N. Marcuvitz, "Waveguide handbook," in Radiation Laboratory Series, L. N. Ridenour Ed., McGraw-Hill Book Co., Inc., New York, N. Y., vol. 10; 1951. See sect. 4.13.

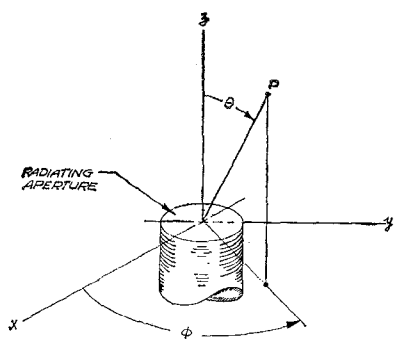


Fig. 1—Spherical coordinate system.

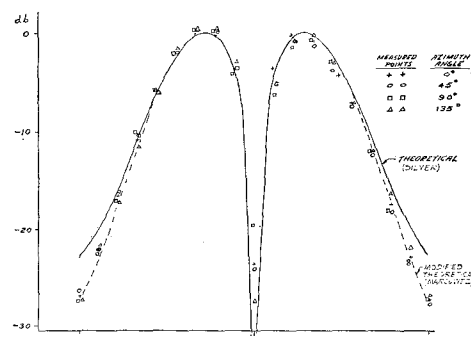
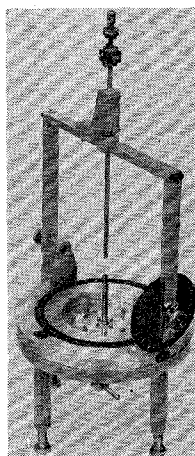
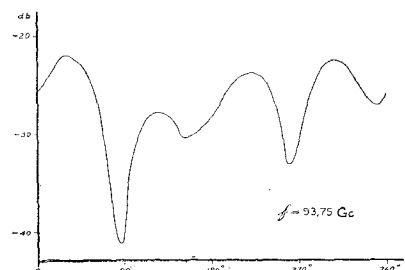
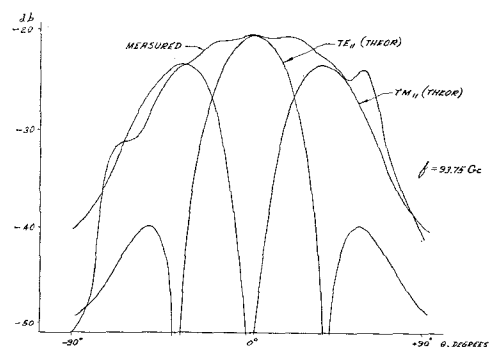
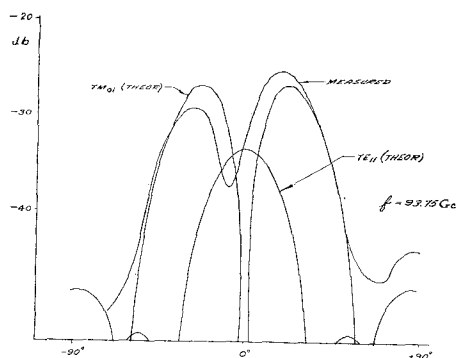
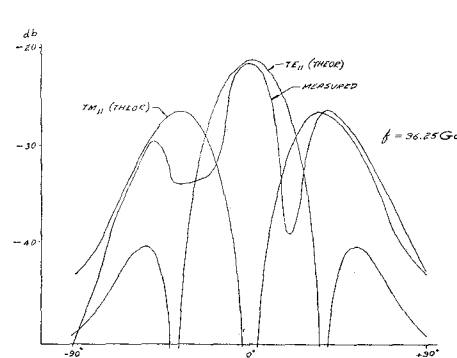
Fig. 2—Elevation patterns,  $TE_{01}$  mode.

Fig. 3—Mode-purity measurement.

Fig. 4—Cross-polarized azimuth pattern,  $\theta = 38^\circ$ .Fig. 5—Cross-polarized elevation pattern,  $\phi = 20^\circ$ .Fig. 6—Cross-polarized elevation pattern,  $\phi = 260^\circ$ .Fig. 7—Cross-polarized elevation pattern,  $\phi = 20^\circ$ .

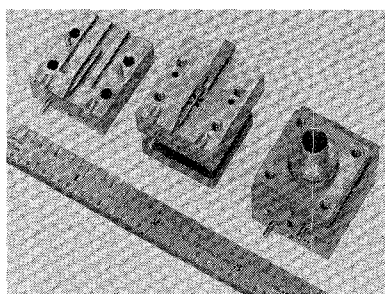


Fig. 8—Experimental four-slot transitions.

The assumption of negligible mode conversion due to the discontinuity at the aperture needs to be justified. In practice, the  $TE_{01}$  mode is in much greater strength than other modes, so that the only conversion effect of significance is from  $TE_{01}$  to other modes. However, the  $TE_{01}$  mode, because of its symmetry and because of the circular symmetry of the radiating boundary, can only couple to higher order  $TE_{0n}$  modes and not to any of the nine propagating modes for whose presence we are looking.

The pattern of the  $TE_{01}$  mode has only an  $E_\phi$  component. It has been plotted in Fig. 2 and compared both with measured values and with values computed by a more accurate formula from Marcuvitz,<sup>6</sup> in which higher modes at the aperture are taken into account. It can be seen that all three agree quite well out to  $60^\circ$ , where the less accurate theory diverges somewhat.

The slight asymmetry in the height of the measured lobes and the filling in of the null at  $\theta=0^\circ$  are indications of the presence of other modes. In particular, the filling in of the null is attributable to the  $TE_{11}$  or  $TE_{12}$  modes which are the only propagating modes having nonzero fields on axis. The choice between these two modes must be made on the basis of further pattern measurements.

It may be noted from (1), (2) and (3) that the only mode with no  $E_\theta$  component is the  $TE_{0n}$  family. Thus, a simple way of measuring the strength of the other possible nine modes in our case was to look at the  $E_\theta$ -component (or cross-polarized) field strength, relative to that of the maximum  $E_\phi$  component due to the  $TE_{01}$  mode.

The apparatus for accomplishing this is shown in Fig. 3. A small rectangular waveguide pickup probe may be oriented to respond to either  $E_\theta$  or  $E_\phi$  and rotated about the aperture in the  $\theta$  or  $\phi$  direction to measure the radiation pattern. A square-law bolometer is used as a power detector. The circular waveguide component under test is attached underneath the carriage to the input end of the short section of radiating pipe.

Some typical measurements on a rectangular to circular transition are shown in Figs. 4-7. Fig. 4 is an  $E_\theta$ -azimuth pattern measured at a value of  $\theta=38^\circ$ . This value of  $\theta$  corresponds to a null in the pattern of the  $TE_{11}$

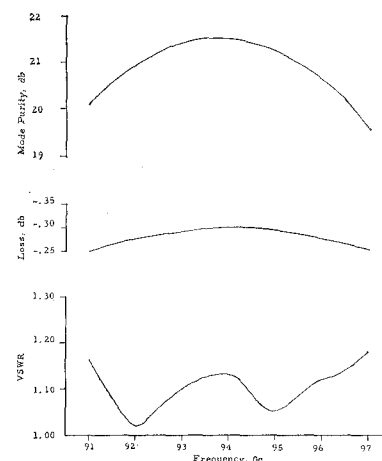


Fig. 9—Performance of transition.

and  $TE_{12}$  modes whose presence was indicated by the filling in of the null in Fig. 2. The signal shown in Fig. 4 indicates the presence of other modes besides the  $TE_{11}$  or  $TE_{12}$ . In order to identify these modes, elevation patterns, Figs. 5 and 6 were measured, one through a peak in the pattern of Fig. 4, the other through a minimum. It can be seen on Fig. 5 that a combination of  $TE_{11}$  and  $TM_{11}$  modes added in phase account nicely for the measured results. The measured peak value of  $TM_{11}$  mode in this plane is 23 db below that of the  $TE_{01}$  mode and, correcting for the difference in gain, indicates that the strength of the  $TM_{11}$  mode in the waveguide is 20.5 db below that of the  $TE_{01}$  mode. This pattern also definitely indicates that it is the  $TE_{11}$  mode which is filling in on axis. Its maximum-on-axis strength was  $-18$  db, and it was approximately linearly polarized so that the power in the  $TE_{11}$  mode was  $-21.5$  db with respect to the  $TE_{01}$  mode. Fig. 6 is an elevation pattern through a null plane in the  $TM_{11}$ -mode pattern, and indicates the presence of some  $TM_{01}$  mode. Note that the  $TM_{01}$  mode adds with the  $TE_{11}$  mode to give an asymmetrical pattern, as is to be expected. The  $TM_{01}$ -mode peak is  $-27$  db, and so its strength in the waveguide is 28.2 db below the  $TE_{01}$  mode. The three spurious modes identified accounted in this case for the major features of the measured patterns. Fig. 7 is measured at the same angle as Fig. 5 but at a higher frequency. It can be seen that the same two modes are present, but their relative phases have changed to a more nearly out-of-phase condition giving a pattern of quite different appearance.

The transition measured here is similar in design to the four-slot transition developed by Lanciani at lower frequencies.<sup>7</sup> (See Fig. 8.) Performance of the final version of this device in the band around 93.75 Gc is shown in Fig. 9.

<sup>7</sup> D. A. Lanciani, "Final Report on Basic Design Criteria for Circular Waveguide Components," Microwave Associates Inc., Boston, Mass., Contract DA-36-039-sc-5518; 1954.

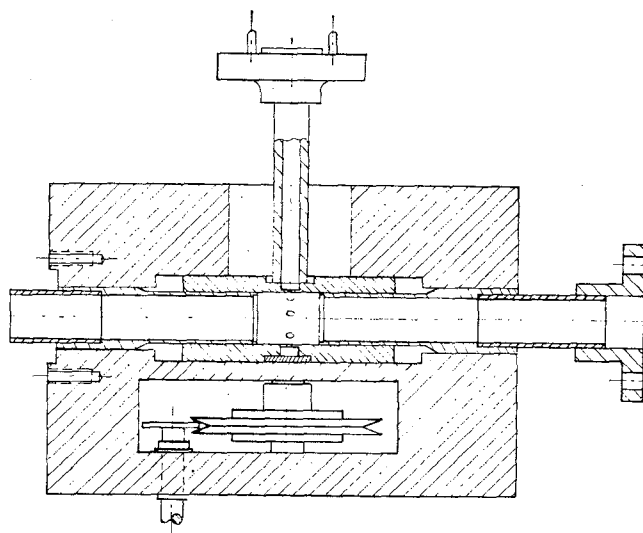


Fig. 10—Slotted line assembly, cutaway.

## STANDING WAVE DETECTOR

In order to sample the standing wave  $TE_{01}$ -mode field in the circular guide, a large gap of several wavelengths was introduced into the waveguide. This gap was enclosed within a closely fitting cylindrical sleeve or slider which could be moved back and forth along the axis of the waveguide. Coupling to the field in the waveguide was accomplished by means of an array of holes evenly spaced about the circumference of the slider which couple out to a rectangular waveguide output. (See Fig. 10.) The problems to be solved were to reduce the effect of the gap in the waveguide to negligible amount; to insure coupling only to the  $TE_{01}$  mode so that residual mode impurity would not interfere with standing wave measurement by spatial beating with the  $TE_{01}$  mode; and to adjust the coupling to a proper value.

The step in the circular guide between the main waveguide and the slider is kept very small by using a minimum wall thickness in the inner guide in the overlap region (a thickness of 0.010 inch was used in the first model to be built). The design is such that the slider does not touch the inner waveguide, but has 0.001- to 0.002-inch clearance in order not to distort the thin-walled section. No choke is needed because of the absence of longitudinal currents in the  $TE_{01}$  mode. The discontinuity is further matched by means of a quarter-wave step in thickness so that the 0.010-inch step was reduced to two 0.005-inch steps. The normalized susceptance of such steps<sup>8</sup> is approximately 0.015, and the expected VSWR of two such steps spaced  $\lambda/4$  should be less than 1.01.

The coupling is accomplished by means of a number of small holes, evenly spaced around the circumference which couple to a waveguide of rectangular cross section

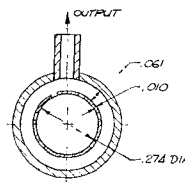


Fig. 11—Output waveguide coupling.

wrapped around the slider. This waveguide is shown in cross section in Fig. 10. The number of coupling holes and the width of this waveguide are determined by the condition that the holes be spaced one guide-wavelength apart in the rectangular guide so that their contributions add in phase and that this guide be an integral number of wavelengths in average circumference. Under these conditions and within the space available, a convenient number of coupling holes was seven, with seven wavelengths being the average circumference of the wrap-around waveguide.

The coupling holes and output waveguide are arranged as shown in Fig. 11. Each coupling hole excites two waves traveling in opposite directions around the loop. Ideally, all these waves add up in phase to produce a maximum at the output guide. If we assume that the junction of the output guide and the ring is equivalent to a symmetrical unmatched Tee junction, its scattering matrix is given by

$$[S] = 1/3 \begin{bmatrix} 1 & 2 & -2 \\ 2 & 1 & 2 \\ -2 & 2 & 1 \end{bmatrix}. \quad (4)$$

The output of the Tee is

$$b_1 = \frac{4}{3} \left( \frac{\sin 7\beta d}{\sin \beta d} \right) \left[ \frac{e^{-7j\beta d}}{1 + \frac{1}{3} e^{-14j\beta d}} \right] \quad (5)$$

where the spacing between slots is taken as  $2d$ , and

$$\beta = 2\pi/\lambda g.$$

Eq. (5) comes from summing all the direct waves, reflected waves and multiply reflected waves incident on the output arms of the Tee. It may be used to compute the frequency sensitivity of the multihole coupler; over the five per cent band of interest, the variation in coupling is less than two per cent.

The coupling holes couple the longitudinal magnetic field in the circular guide to the transverse magnetic field in the wrap-around waveguide. Because of the seven holes, only the  $TE_{01}$  mode of the noncutoff  $TE_{mn}$  family has sufficient symmetry to be coupled out. TM modes having no longitudinal magnetic field cannot couple via magnetic field. The  $TM_{01}$  mode has sufficient symmetry, and could couple via the electric field component except that the wave set up in the ring wave-

<sup>8</sup> L. B. Felsen and W. K. Karn, "Network Properties of Discontinuities in Multimode Circular Waveguide," *Microwave Res. Inst.*, Polytechnic Inst. of Brooklyn, Brooklyn, N. Y., Res. Rept. No. PIB MRI-803-60, Contract DA36-039-sc-78001; 1960.

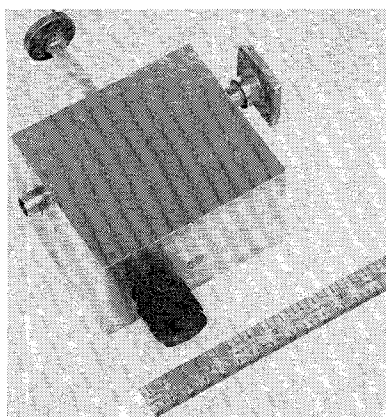


Fig. 12—Standing wave detector.

guide would have a null rather than a maximum at the output port. Thus, the slider samples only the  $TE_{01}$  mode.

The coupling coefficient may be calculated using Béthe's small-hole theory,<sup>9</sup> and including a correction for wall thickness,

$$C_{db} = 10 \log_{10} \left[ 2.65 \frac{\pi \lambda g_{01}}{ab \lambda g_{10}} \frac{l^6}{r_0^4} \right] - 16.3 \frac{t}{l} \sqrt{1 - \left( \frac{3.413l}{\lambda_0} \right)^2} \quad (6)$$

where

$\lambda g_{01}$  = the wavelength in the circular guide,

$\lambda g_{10}$  = the wavelength in the rectangular guide,

$a$  and  $b$  = the width and height of the rectangular guide,

$r_0$  = the radius of the circular guide,

$l$  = the hole radius,

$t$  = the wall thickness.

It is desirable to couple out as much power as possible in order to improve the output SNR. The maximum coupling is limited by the discontinuity allowable in the main waveguide. The seven holes act mainly as shunt susceptance in the main waveguide which may be calculated by the small-hole approximate theory.<sup>9</sup> It can be shown<sup>10</sup> than an error of less than 2° in minimum position and one per cent in VSWR is obtained if the normalized susceptance of the coupling holes is less than 0.14. Using this value, we obtained a maximum permissible radius for the coupling holes of 0.635 mm, which resulted in a theoretical output coupling of -16.9 db.

An experimental model was built according to the previous theory (see Fig. 12). A gap of approximately  $2 \lambda g$  was opened in the main waveguide, to permit adequate sampling of the field. Measurements of the

<sup>9</sup> R. E. Collin, "Field Theory of Guided Waves," McGraw-Hill Book Co. Inc., New York, N. Y.; 1960. See especially sect. 7.3.

<sup>10</sup> A. J. Simmons, "3-MM. Waveguide Components," U. S. Army Signal Research and Development Laboratory, Fort Monmouth, N. J., Second Quart. Rept. Contract No. DA36-039-sc-88979; 1962. See especially pp. 19-23.

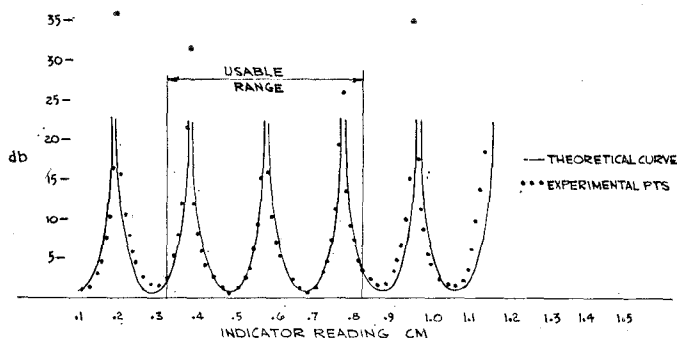


Fig. 13—Typical standing wave pattern.

standing wave pattern were made with a short circuit at the end of the line and compared with the theoretical pattern (see Fig. 13). It is apparent that some perturbation effects occur as the coupling holes get near the edge of the gap, so that this slotted line is only usable for a range of one guide-wavelength near the center of travel. In a second model under construction, the gap is made somewhat wider to permit more usable range.

The residual VSWR was evaluated by use of a sliding load of actual VSWR 1.17. Maximum VSWR measured was 1.20, minimum, 1.15, indicating a residual VSWR for the standing wave detector of 1.02.

The standing wave detector itself did not appreciably affect the mode purity of the wave traveling through it. Coupling to the output arm was approximately -15 db, reasonably close to the -16.9 db calculated. Coupling to modes other than the  $TE_{01}$  is small as evidenced by approximately 20-db mode purity measured when feeding into the output arm and exciting a  $TE_{01}$  mode in the slider.

Some  $TE_{02}$ -mode excitation was evident at 97 Gc (the cutoff frequency for this mode in the slider section was 96.5 Gc.) In the second model, the slider diameter was reduced slightly to push this cutoff frequency higher, but there is still an upper limit of about 98 Gc on this design.

#### VARIABLE ATTENUATOR

Design of a variable attenuator for the  $TE_{01}$  mode presents certain difficulties since the electric field in the waveguide is difficult to attack with lossy dielectrics because of its location and symmetry. In addition, it is difficult to remove heat efficiently from any material inserted into the waveguide.

It has been observed in accordance with theory<sup>6</sup> that the radiating aperture of the  $TE_{01}$ -mode waveguide was well matched to space. An attenuator based on allowing energy to radiate from the waveguide into an absorbing enclosure was therefore designed. The basic principle is to break the waveguide with a gap of variable length which then leaks various amounts of energy into the absorbing enclosure. The major problem occurs at the moment of separation of the waveguide. A slot with large series reactance is obtained when the gap is ap-

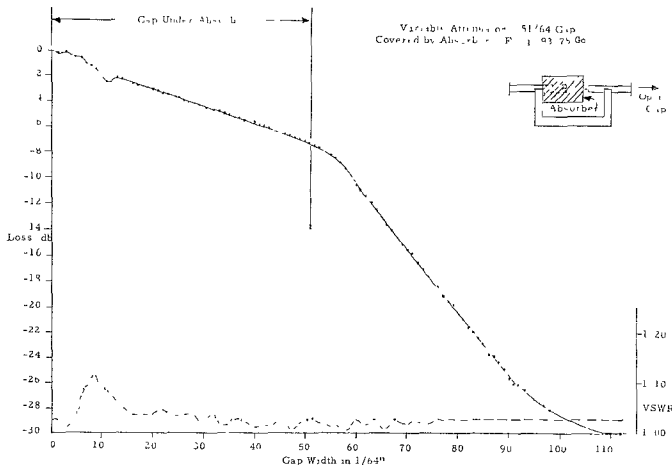


Fig. 14—Experimental attenuator.

proximately one-half wavelength long. The maximum value of VSWR observed which was caused by this reactance was 1.6. In order to break up this resonant effect and reduce the VSWR, four approximately quarter-wave interlocking teeth were machined in the mating ends of the pipe. By this means and by covering the initial portion of the gap with a lossy dielectric material, the maximum VSWR was reduced to 1.12. Performance of the experimental prototype is shown in Fig. 14. As can be seen, 30-db attenuation is obtained for somewhat less than two inches of travel. By varying the height of the teeth somewhat, the maximum VSWR has recently been further reduced at the center of the band to 1.08. Fig. 15 is a cutaway view of a complete attenuator under construction based on this principle. A telescoping section permits sliding of one section with respect to the other without movement of the ends of the waveguide.

#### OTHER COMPONENTS

Other components which have been built to operate at 3.2 mm are directional couplers, flexible waveguide and fixed bends, and rotary joints. The latter are electrically simple because of the circular symmetry of the mode and the absence of a need for chokes at a break in the waveguide. Fig. 16 is a sketch of a typical rotary joint. Waveguide bends present a problem because of degeneracy and mode conversion between the  $TE_{01}$  and  $TM_{11}$  modes. This degeneracy may be removed by corrugating the inner wall of the waveguide, as has been pointed out by many workers in this field. The method we have used is to machine a corrugated circular mandrel, bend it to the required angle and then coat it with copper by the electroforming process. The mandrel is then dissolved, leaving the waveguide bend. Flexible waveguides may be made in this manner by using only a thin copper layer which is flexible. The flexible guide may be protected by a suitable rubber jacket. (See Fig. 17.) Ninety-degree bends of 3-inch radius with negligible mode conversion have also been obtained by this technique (see Fig. 18).

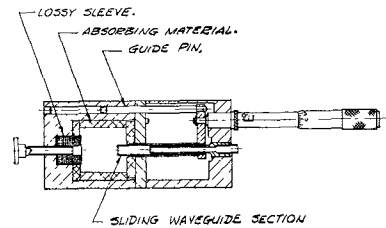


Fig. 15—Variable attenuator.

Directional couplers between the  $TE_{01}$ -mode circular guide and the  $TE_{10}$  mode in rectangular guide have been built by various groups.<sup>11,12</sup> They are most readily made by selecting waveguide sizes so that phase velocities for the two modes are matched. Multiple coupling holes provide the necessary mode purity and directivity. By coupling the longitudinal magnetic field at the side wall in the rectangular waveguide to the longitudinal magnetic field in the circular guide, coupling to the  $TE_{mn}$  modes alone is effected. Discrimination against all but the  $TE_{01}$  mode is accomplished by making the coupling region sufficiently long.<sup>11</sup> In the present case, the  $TE_{31}$  mode is closest in phase velocity to the  $TE_{01}$ ; therefore, we make the coupler sufficiently long so that

$$(\beta_{01} - \beta_{31}) \frac{2N + 1}{2} d = \pi$$

where

$\beta_{01}$  = the propagation constant for the  $TE_{01}$  mode,  
 $\beta_{31}$  = the propagation constant for the  $TE_{31}$  mode,  
 $N$  = the number of slots,  
 $d$  = the slot spacing.

This leads to an over-all length of about  $2\frac{1}{2}$  inches with about 63 slots spaced  $\lambda g/4$ . It turns out that the slots are none too many for the desired 10-db coupling.

The coupling coefficients of the individual slots were calculated using small-hole theory as before. The distribution used for the coupling coefficients was a superposed binomial distribution, with coupling varying in the ratio 1:6:15:21:21 · · · 21:15:6:1 to obtain a proper taper at the ends of the array.

In order to match phase velocity, the  $a$  dimension of the rectangular guide must be chosen to give the same cutoff frequency as that of the circular guide. This turns out to require  $a = 0.1025$  inch. However, the coupling hole susceptance loads the rectangular waveguide more than it does the circular waveguide, giving a calculated net phase difference of  $1.2^\circ$  per slot, so the calculated  $a$  dimension of the rectangular guide had to be reduced still further, to 0.100 inch. In experimental tests an  $a$  dimension of 0.098 inch gave slightly greater coupling than 0.100 inch.

<sup>11</sup> S. E. Miller, "Coupled wave theory and waveguide application," *Bull. Sys. Tech. J.*, vol. 33, pp. 661-719; May, 1954.

<sup>12</sup> A. Jaumann, "Über Richtungskoppler zur Erzeugung der  $H_{01}$ -Welle im runden Hohlleiter," *Arch. Elekt. Übertragung* vol. 10, pp. 440-446; October, 1958.

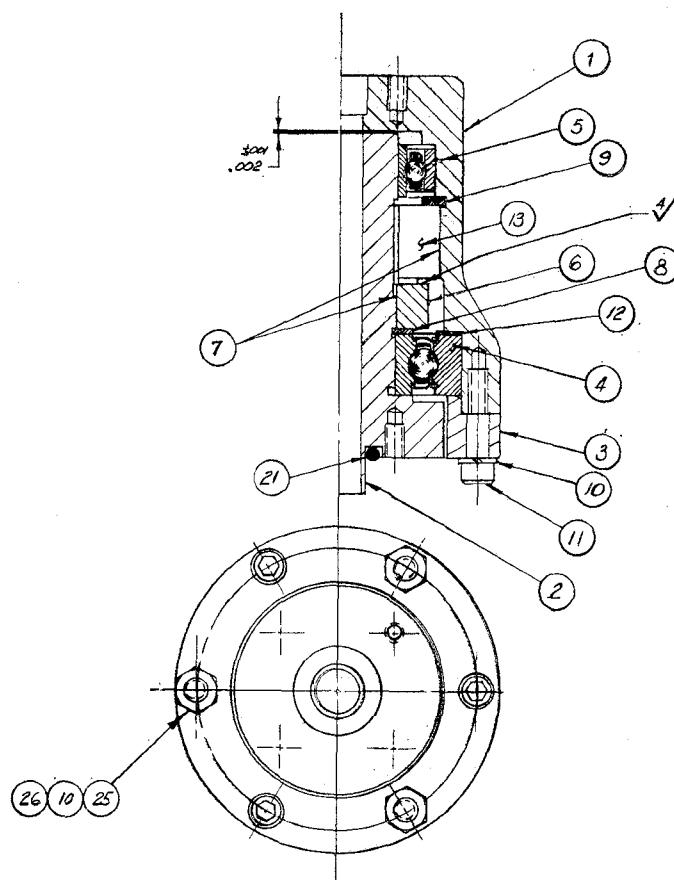


Fig. 16—Rotary joint assembly.

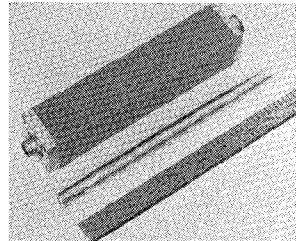


Fig. 17—Flexible waveguide with aluminum mandrel.

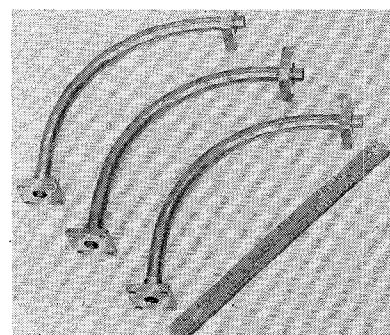


Fig. 18—Three circular waveguide bends.

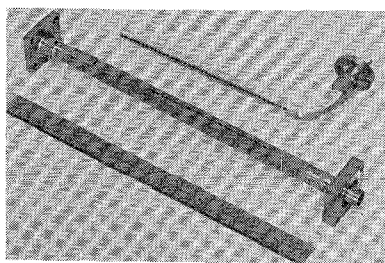


Fig. 19—Experimental model of directional coupler.

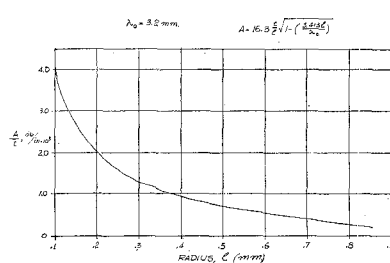
Fig. 20—Attenuation of a small circular hole radius  $l$ .

Fig. 19 is a picture of the unassembled coupler. It was found that the wall thickness was quite critical in obtaining a precise value of coupling. This is understandable. Fig. 20 is a plot of the wall thickness term in (6). For the holes used in the coupler, change in  $t$  of 0.001 inch gives a change of coupling of approximately 1 db.

Results obtained with these couplers over a five-per cent band are typically:

coupling variation	9.8–10.1 db
directivity	greater than 25 db
VSWR, circular guide	less than 1.05
VSWR, rectangular guide	less than 1.15.

The mode purity of the wave passing through the coupler was negligibly disturbed by the coupling holes.

## CONCLUSION

Although care must be exercised in maintaining mode purity it appears feasible to construct many components to operate in the circular electric  $TE_{01}$  mode. Test and operational systems operating entirely in this mode in millimeter region appear a possibility for the near future. Major components still lacking are nonreciprocal ferrite devices on which some research has been carried out, and detectors of various kinds.

# A Range of 2 and 1 Millimeter Waveguide Components\*

R. MEREDITH† AND G. H. PREECE†

**Summary**—A variety of components have been made in waveguides RG136 and RG139 by techniques which include the use of extruded waveguide, copper-gold eutectic bonding, precision milling and, in particular, of electroforming. Performances of several RG136 components are given, together with the loss in RG139 waveguide and in oversized guide tapered from RG139.

Ferrite devices, including isolators, 3 port switches and amplitude modulators, using Ferramic R1, have been quite successful. A typical isolator has an insertion loss of  $1\frac{1}{4}$  db and an isolation of 30 db, magnetically tunable over at least 133 to 145 Gc.

An RG136 slotted line, at a coupling ratio of 20 db, has an inherent mismatch of 1.05 with good reproducibility over the  $2\frac{1}{2}$  wavelengths traverse of the one-mil Wollaston wire probe. The main waveguide is milled and broached from brass and gold plated.

Electroformed matched hybrid Tees in RG136 split power to  $\pm\frac{1}{4}$  db, have a discrimination of 30 db, a loss of  $1\frac{1}{4}$  db and a match looking into any arm of better than 1.4.

Rotary and flap-type attenuators, phase shifters, variable short circuits, matching units, crystal diodes and their mounts, bolometers and dry calorimeters, etc., have been made, and for transmission over moderate distances the vastly overmoded  $TE_{01}$  waveguide was used.

## INTRODUCTION

TO AID a program of plasma diagnostics by the United Kingdom Atomic Energy Authority and, in particular, to facilitate the development of

sensitive receivers<sup>1</sup> at 140 Gc and 280 Gc, a variety of components have been developed in waveguides RG136 and RG139, but no attempt has been made to make a complete range of components or to broadband them.

Fabrication techniques<sup>2</sup> include the use of the drawn waveguide, copper-gold eutectic bonding, precision milling, and especially, of electroforming. In several cases spark erosion techniques are used.

Dimensional tolerances are small—on the stainless steel mandrels usually used in the electroforming they are normally 0.1 or 0.2 mil, with surface finishes of 5 microinches or better.

Waveguide wall losses are high, measured attenuations being 2.73 db/ft at 140 Gc in RG136 guide and  $6\frac{3}{4}$  db/ft at 280 Gc in RG139, both waveguides being drawn down from extruded coin silver RG99 waveguide. The comparable theoretical attenuations are 1.56 and 4.22 db/ft, respectively.

Despite these heavy attenuations and the small dimensions involved, quite useable components on conventional lines can be made in these waveguides, as the following examples will show.

<sup>1</sup> R. Meredith and F. L. Warner, "Superheterodyne Radiometers for Use at 70 Gc and 140 Gc," presented at the IRE Millimeter and Submillimeter Conference, Orlando, Fla.; January, 1963.

<sup>2</sup> A. F. Harvey, "Mechanical design and manufacture of microwave structures," IEEE TRANSACTIONS ON MICROWAVE THEORY AND TECHNIQUES, vol. MIT-7, pp. 402-422; October, 1959.

\* Received January 21, 1963; revised manuscript received April 29, 1963.

† Royal Radar Establishment, Great Malvern, Worcs., England.